J|A|C|S COMMUNICATIONS

Published on Web 10/30/2009

# Russian-Doll-Type Metal Carbide Endofullerene: Synthesis, Isolation, and Characterization of $Sc_4C_2@C_{80}$

Tai-Shan Wang,[†,‡] Ning Chen,[†] Jun-Feng Xiang,[†] Bao Li,[†] Jing-Yi Wu,[†] Wei Xu,[†] Li Jiang,[†] Kai Tan,[§] Chun-Ying Shu,*[,†] Xin Lu,*[,§] and Chun-Ru Wang*[,†]

*Beijing National Laboratory for Molecular Sciences, Institute of Chemistry, Beijing 100080, China, Graduate School of the Chinese Academy of Sciences, Beijing 100049, China, and State Key Laboratory of Physical Chemistry of Solid Surfaces & Center for Theoretical Chemistry, College of Chemistry and Chemical Engineering, Xiamen University, Xiamen 361005, China*

Received September 14, 2009; E-mail: shucy@iccas.ac.cn; xinlu@xmu.edu.cn; crwang@iccas.ac.cn

Endohedral metallofullerenes have broadened the range of fullerenes by virture of their novel structures and promising applications.[1,2] To date, the compositions of the endohedral clusters vary, including one metal atom, two metal atoms, and trimetallic nitride, metal carbide, and metal oxide clusters, etc.[1−6] Because endofullerenes have so many abundant endohedral clusters, they can be provided with intricate structures and properties, such as the quantum gyroscope $Sc_2C_2@C_{84}$ as well as $Sc_4(\mu\text{-}O_2)@C_{80}$ with a distorted tetrahedral scandium oxide cluster inside a carbon cage.[6,7] For a long time, inorganic nesting polyhedra and carbon onions have attracted much attention because of their distinctive endohedral architectures.[8] However, metallofullerenes with nesting structures have not been available.[1,2] Recently, the structure of $Sc_4C_2@C_{80}$-$I_h$ was predicted by density functional theory (DFT) calculations, which revealed that $C_2@Sc_4@C_{80}$-$I_h$ is the more realistic formula for $Sc_4C_{82}$.[9] Herein, we report the synthesis, isolation, and characterization of $Sc_4C_{82}$ by means of mass spectrometry (MS) and UV−vis, FTIR, and $^{13}C$ NMR spectroscopy measurements in combination with DFT calculations and show that the synthesized $Sc_4C_{82}$ is indeed $Sc_4C_2@C_{80}$-$I_h$ or, more exactly, $C_2@Sc_4@C_{80}$-$I_h$, i.e., a $C_2$ unit surrounded by a $Sc_4$ tetrahedron then encaged in an icosahedral $C_{80}$ ($C_{80}$-$I_h$) cage.

$Sc_4C_{82}$ was prepared by the Krätschmer−Huffman arc discharge method and isolated by two-stage high performance liquid chromatography (HPLC) [see the Supporting Information (SI)]. The soot was promptly Soxhlet-extracted with toluene. HPLC using two columns, namely, Buckyprep and Buckyprep-M, was employed to isolate and purify the $Sc_4C_{82}$, respectively. The purity of the sample was confirmed by HPLC analysis and the MALDI−TOF mass spectrum (Figure 1). The MALDI−TOF mass spectrum exhibits a strong molecular ion peak at *m*/*z* 1164, accounting for the production of $Sc_4C_{82}$.

Figure 2 presents the $^{13}C$ NMR spectrum of $Sc_4C_{82}$ in $CS_2$ at 293 K. Two signals at 137.8 and 144.7 ppm in a 1:3 intensity ratio can be clearly observed. It is unreasonable to identify the molecular structure as $Sc_4@C_{82}$, as no $C_{82}$ cage can satisfy this $^{13}C$ NMR spectral pattern. Instead, the spectrum is fully consistent with the $C_{80}$-$I_h$ cage, which has two unique carbon atoms (the triphenylenic and corannulenic sites) in a 1:3 atomic ratio. Although the $Sc_4C_2$ endocluster may disturb the chemical environment of the carbon atoms of the $C_{80}$ cage, the influence can be markedly reduced via intramolecular dynamics and cage rotations.[9,11] To our knowledge, two distinct $^{13}C$ NMR signals of the $C_{80}$-$I_h$ cage were also observed for $Sc_3N@C_{80}$-$I_h$ (137.24 and 144.57 ppm),[3a] $Lu_3N@C_{80}$-$I_h$ (137.4 and 144.0 ppm),[10] $CeSc_2N@C_{80}$-$I_h$ (135.90 and 142.85 ppm),[11] and $Sc_3C_2@C_{80}$-$I_h$ (138.9 and 145.6 ppm).[5a] As shown in Figure 2, the DFT-predicted $^{13}C$ NMR spectrum (with signals at 137.7 and 143.7 ppm) for the $Sc_4C_2@C_{80}$-$I_h$ structural model[9] (Figure 3) agrees well with the experimental $^{13}C$ NMR spectrum. The $^{13}C$ NMR chemical shifts of $C_2$ units within the endocluster, which were calculated to

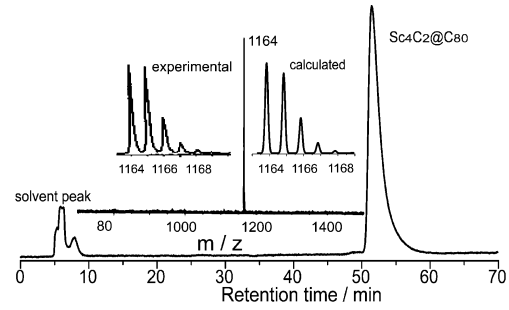


***Figure 1.*** HPLC trace of $Sc_4C_2@C_{80}$-$I_h$ in a Buckyprep column. The inset shows the positive-ion MALDI-TOF mass spectrum as well as the experimental and calculated isotope distributions of $Sc_4C_2@C_{80}$-$I_h$.

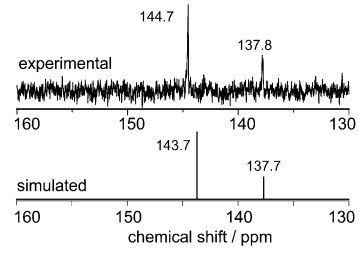


***Figure 2.*** (top) Experimental ($CS_2$, 150 MHz) and (bottom) simulated $^{13}C$ NMR spectra of the $C_{80}$-$I_h$ cage in $Sc_4C_2@C_{80}$-$I_h$. $D_2O$ inside of a capillary was used as an internal lock.

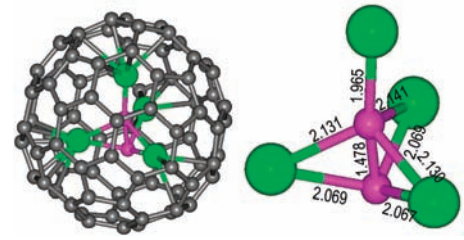


***Figure 3.*** (left) DFT-optimized structure of $Sc_4C_2@C_{80}$-$I_h$ and (right) calculated Sc−C and C−C bond lengths (Å) in the encaged $Sc_4C_2$ moiety. Green balls represent the Sc atoms and purple balls the carbon atoms of the inner carbide moiety.

[†] Institute of Chemistry.
[‡] Graduate School of the Chinese Academy of Sciences.
[§] Xiamen University.



10.1021/ja9077842 CCC: $40.75 

***Table 1.*** Experimental and DFT-Calculated Redox Potentials (V) of $Sc_4C_2@C_{80}$-$I_h$

| | $_{ox}E_2$ | $_{ox}E_1$ | $_{red}E_1$ | $_{red}E_2$ |
|---|---|---|---|---|
| exptl[a] | 1.10 | 0.40 | −1.16 | −1.65 |
| DFT[b] | 1.30 | 0.32 | −1.33 | −2.02 |

[a] Values are given vs $Fc/Fc^+$ and were obtained in *o*-dichlorobenzene containing 0.1 M $TBAPF_6$ at a glassy carbon working electrode via CV at a scan rate of 100 mV $s^{-1}$. [b] From ref 9.

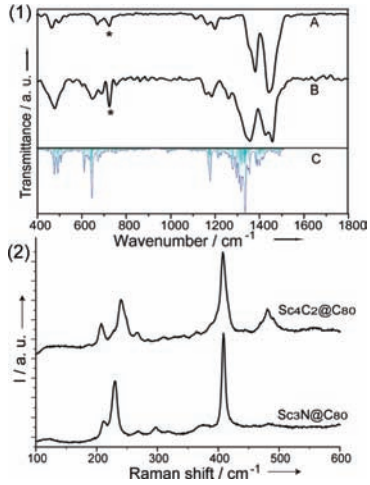


***Figure 4.*** (1) FTIR spectra of (A) $Sc_3C_2@C_{80}$-$I_h$ and (B) $Sc_4C_2@C_{80}$-$I_h$ along with (C) the simulated IR spectrum of $Sc_4C_2@C_{80}$-$I_h$. The asterisks show the solvent peaks. (2) Low-energy Raman spectra of $Sc_4C_2@C_{80}$-$I_h$ and $Sc_3N@C_{80}$-$I_h$ (laser wavelength 633 nm).

appear at 226.1 and 326.7 ppm, were not detected because of the spin−rotation interaction and low signal-to-noise ratio.[5e,9]

Previous DFT computations have shown that $Sc_4C_2@C_{80}$-$I_h$ has a valence state of $[C_2]^{6-}@[Sc^{3+}]_4@[C_{80}\text{-}I_h]^{6-}$ with a wide HOMO−LUMO gap.[9] Table 1 lists the redox potentials of $Sc_4C_2@C_{80}$-$I_h$ obtained by cyclic voltammetry (CV) and DFT computations. The measured electrochemical band gap of 1.56 eV, along with the DFT prediction (1.65 eV), indicates that $Sc_4C_2@C_{80}$-$I_h$ is a very stable metallofullerene.

The FTIR spectra of $Sc_4C_2@C_{80}$-$I_h$ and $Sc_3C_2@C_{80}$-$I_h$ and the DFT-simulated IR spectrum of $Sc_4C_2@C_{80}$ are shown in Figure 4. First of all, the experimental FTIR spectrum of $Sc_4C_2@C_{80}$ agrees well with the previously DFT-computed IR spectrum[9] of $Sc_4C_2@C_{80}$-$I_h$ (Figure 4). The peaks ranging from 1600 to 1000 $cm^{-1}$ can be considered as a group of tangential cage modes of the outer carbon cage.[12] The characteristic vibrations of the tangential cage modes are approximately at 1184, 1359, 1459, and 1513 $cm^{-1}$ for $Sc_4C_2@C_{80}$-$I_h$. These tangential cage modes of $Sc_4C_2@C_{80}$-$I_h$ exhibit quite a degree of resemblance to those of the well-known species $M_3N@C_{80}$-$I_h$ (M = Sc, Dy, Tm, Gd).[12] The vibrational frequency at 480 $cm^{-1}$ can be assigned to the radial cage mode.[12] Signals at 600, 645, and 688 $cm^{-1}$ represent asymmetric $Sc-C_{carbide}$ stretching vibrations, indicating that there are three kinds of $Sc-C_{carbide}$ stretching modes in $Sc_4C_2@C_{80}$-$I_h$. This assignment is in line with the calculated structure, which presents three groups of $Sc-C_{carbide}$ bonds according to the various bond lengths (Figure 3).

The low-energy Raman spectrum of $Sc_4C_2@C_{80}$-$I_h$ (Figure 4) shows a resemblance to those of $Sc_3N@C_{80}$-$I_h$, $Dy_3N@C_{80}$-$I_h$, and $Sc_3CH@C_{80}$-$I_h$.[13] The line groups at ∼481 and 240 $cm^{-1}$ are characteristic of the $A_g(1)$- and $H_g(1)$-derived cage modes of $C_{80}$-$I_h$, respectively.[13] It should be noted that the cage modes show obvious splittings, such as those of the $A_g(1)$-derived modes at 470, 481, and 490 $cm^{-1}$ and the $H_g(1)$-derived cage modes at 230, 240, and 249 $cm^{-1}$. Such big splittings suggest that distortions in the icosahedral $C_{80}$ cage result from presence of the big $Sc_4C_2$ cluster.[13c] Two groups of lines at ∼208 and 407 $cm^{-1}$ also give splittings caused by the complex structure of the $Sc_4C_2$ cluster (Figure 3). The medium line at 208 $cm^{-1}$ and weak line at 187 $cm^{-1}$ can be assigned to the $Sc_4C_2$ translation modes, and the group of lines around 407 $cm^{-1}$ represents the $\nu_s(Sc-C)$ modes of the $Sc_4C_2$ moiety.[13] Therefore, the Raman spectral analysis confirms the $Sc_4C_2@C_{80}$-$I_h$ structure.

In conclusion, for the first time we have produced stable $Sc_4C_2@C_{80}$-$I_h$ and characterized it as a metal carbide endofullerene by FTIR and Raman spectra in combination with DFT calculations. Furthermore, DFT calculations have demonstrated that this molecule has a Russian-doll-type structure, $C_2@Sc_4@C_{80}$. To the best of our knowledge, $Sc_4C_2@C_{80}$-$I_h$ is the first metallofullerene that exhibits a Russian-doll nesting structure.

**Acknowledgment.** C.-R.W. thanks the 973 Program (2006CB300402) and NSFC (20821003). X.L. thanks NSFC (20673088, 20425312, 20721001, and 20423002), the 973 Program (2007CB815307), and Xiamen University (Mingjiang Professorship).

**Supporting Information Available:** Experimental details, UV−vis−NIR spectrum, and CV and HPLC data. This material is available free of charge via the Internet at http://pubs.acs.org.

## References

(1) Shinohara, H. *Rep. Prog. Phys.* **2000**, *63*, 843.
(2) (a) Dunsch, L.; Yang, S. F. *Phys. Chem. Chem. Phys.* **2007**, *9*, 3067. (b) Dunsch, L.; Yang, S. F. *Small* **2007**, *3*, 1298.
(3) (a) Stevenson, S.; Rice, G.; Glass, T.; Harich, K.; Cromer, F.; Jordan, M. R.; Craft, J.; Hadju, E.; Bible, R.; Olmstead, M. M.; Maitra, K.; Fisher, A. J.; Balch, A. L.; Dorn, H. C. *Nature* **1999**, *401*, 55. (b) Wang, C. R.; Kai, T.; Tomiyama, T.; Yoshida, T.; Kobayashi, Y.; Nishibori, E.; Takata, M.; Sakata, M.; Shinohara, H. *Angew. Chem., Int. Ed.* **2001**, *40*, 397.
(4) (a) Yang, H.; Lu, C. X.; Liu, Z. Y.; Jin, H. X.; Che, Y. L.; Olmstead, M. M.; Balch, A. L. *J. Am. Chem. Soc.* **2008**, *130*, 17296. (b) Huang, H. J.; Yang, S. H.; Zhang, X. X. *J. Phys. Chem. B* **2000**, *104*, 1473. (c) Zuo, T. M.; Xu, L. S.; Beavers, C. M.; Olmstead, M. M.; Fu, W. J.; Crawford, D.; Balch, A. L.; Dorn, H. C. *J. Am. Chem. Soc.* **2008**, *130*, 12992. (d) Popov, A. A.; Dunsch, L. *J. Am. Chem. Soc.* **2008**, *130*, 17726. (e) Mercado, B. Q.; Beavers, C. M.; Olmstead, M. M.; Chaur, M. N.; Walker, K.; Holloway, B. C.; Echegoyen, L.; Balch, A. L. *J. Am. Chem. Soc.* **2008**, *130*, 7854.
(5) (a) Iiduka, Y.; Wakahara, T.; Nakahodo, T.; Tsuchiya, T.; Sakuraba, A.; Maeda, Y.; Akasaka, T.; Yoza, K.; Horn, E.; Kato, T.; Liu, M. T. H.; Mizorogi, N.; Kobayashi, K.; Nagase, S. *J. Am. Chem. Soc.* **2005**, *127*, 12500. (b) Nishibori, E.; Terauchi, I.; Sakata, M.; Takata, M.; Ito, Y.; Sugai, T.; Shinohara, H. *J. Phys. Chem. B* **2006**, *110*, 19215. (c) Tan, K.; Lu, X. *J. Phys. Chem. A* **2006**, *110*, 1171. (d) Taubert, S.; Straka, M.; Pennanen, T. O.; Sundholm, D.; Vaara, J. *Phys. Chem. Chem. Phys.* **2008**, *10*, 7158. Kato, T. *J. Mol. Struct.* **2007**, *838*, 84. (e) Yamazaki, Y.; Nakajima, K.; Wakahara, T.; Tsuchiya, T.; Ishitsuka, M. O.; Maeda, Y.; Akasaka, T.; Waelchli, M.; Mizorogi, N.; Nagase, S. *Angew. Chem., Int. Ed.* **2008**, *47*, 7905.
(6) (a) Stevenson, S.; Mackey, M. A.; Stuart, M. A.; Phillips, J. P.; Easterling, M. L.; Chancellor, C. J.; Olmstead, M. M.; Balch, A. L. *J. Am. Chem. Soc.* **2008**, *130*, 11844. (b) Valencia, R.; Rodriguez-Fortea, A.; Stevenson, S.; Balch, A. L.; Poblet, J. M. *Inorg. Chem.* **2009**, *48*, 5957.
(7) Krause, M.; Hulman, M.; Kuzmany, H.; Dubay, O.; Kresse, G.; Vietze, K.; Seifert, G.; Wang, C.; Shinohara, H. *Phys. Rev. Lett.* **2004**, *93*, 137403.
(8) (a) Alvarez, S. *Dalton Trans.* **2006**, 2045. (b) Alvarez, S. *Dalton Trans.* **2005**, 2209. (c) Ugarte, D. *Nature* **1992**, *359*, 707.
(9) Tan, K.; Lu, X.; Wang, C. R. *J. Phys. Chem. B* **2006**, *110*, 11098.
(10) Iezzi, E. B.; Duchamp, J. C.; Fletcher, K. R.; Glass, T. E.; Dorn, H. C. *Nano Lett.* **2002**, *2*, 1187.
(11) Wang, X. L.; Zuo, T. M.; Olmstead, M. M.; Duchamp, J. C.; Glass, T. E.; Cromer, F.; Balch, A. L.; Dorn, H. C. *J. Am. Chem. Soc.* **2006**, *128*, 8884.
(12) (a) Krause, M.; Dunsch, L. *ChemPhysChem* **2004**, *5*, 1445. (b) Krause, M.; Liu, X. J.; Wong, J.; Pichler, T.; Knupfer, M.; Dunsch, L. *J. Phys. Chem. A* **2005**, *109*, 7088. (c) Krause, M.; Wong, J.; Dunsch, L. *Chem.—Eur. J.* **2005**, *11*, 706. (d) Krause, M.; Dunsch, L. *Angew. Chem., Int. Ed.* **2005**, *44*, 1557. (e) Yang, S. F.; Dunsch, L. *Chem.—Eur. J.* **2006**, *12*, 413.
(13) (a) Krause, M.; Kuzmany, H.; Georgi, P.; Dunsch, L.; Vietze, K.; Seifert, G. *J. Chem. Phys.* **2001**, *115*, 6596. (b) Yang, S. F.; Troyanov, S. I.; Popov, A. A.; Krause, M.; Dunsch, L. *J. Am. Chem. Soc.* **2006**, *128*, 16733. (c) Krause, M.; Ziegs, F.; Popov, A. A.; Dunsch, L. *ChemPhysChem* **2007**, *8*, 537.

JA9077842